coatings

MDPI

Article

Near Infrared Sensor to Determine Carbon Dioxide Gas Based on Ionic Liquid

María Dolores Fernández-Ramos [1,2,*], Fátima Mirza-Montoro [1], Luis Fermín Capitán-Vallvey [1,2] and Isabel María Pérez de Vargas-Sansalvador [1,2]

[1] ECsens, Department of Analytical Chemistry, University of Granada, 18071 Granada, Spain; fatima1992@correo.ugr.es (F.M.-M.); lcapitan@ugr.es (L.F.C.-V.); isabelpdv@ugr.es (I.M.P.d.V.-S.)
[2] Unit of Excellence in Chemistry Applied to Biomedicine and the Environment, University of Granada, 18071 Granada, Spain
* Correspondence: mdframos@ugr.es

Abstract: In this study we present an NIR carbon dioxide gas sensor based on an inner filter process that includes an ionic liquid (IL), 1-ethyl-3-methylimidazolium tetrafluoroborate (EMIMBF$_4$), to improve its stability, dynamic behavior and lifetime, which are usually the main drawbacks with these sensors. The presence of CO_2 causes a displacement of a simple boron-dipyrromethene-type fluorophore, azaBODIPY, as the pH indicator towards its acid form. This increases the emission intensity of Cr(III)-doped gadolinium aluminium borate (GAB) as the luminophore. The characterization of the prepared sensor was carried out and a discussion of the results is presented. The response and recovery times improved considerably, 23 and 49 s, respectively, with respect to the sensor without IL, at 60 and 120 s, respectively,. Additionally, the measurement range is extended when using IL, able in this case to measure in the complete range up to 100% CO_2; without IL the measurement range is limited to 60% CO_2. The detection limit ranges from 0.57% CO_2 without IL to 0.26% CO_2 when IL is added. The useful lifetime of the sensing membrane was 20 days for membranes with IL and only 6 days for membranes without IL, with the sensor always kept in the dark and without the need to maintain a special atmosphere.

Keywords: NIR; ionic liquids; carbon dioxide determination; fluorescent sensor; azaBODIPY

Citation: Fernández-Ramos, M.D.; Mirza-Montoro, F.; Capitán-Vallvey, L.F.; Pérez de Vargas-Sansalvador, I.M. Near Infrared Sensor to Determine Carbon Dioxide Gas Based on Ionic Liquid. *Coatings* **2021**, *11*, 163. https://doi.org/10.3390/coatings11020163

Academic Editor: Octavian Buiu
Received: 20 December 2020
Accepted: 27 January 2021
Published: 30 January 2021

1. Introduction

So-called green solvent ionic liquids are salts that remain as a liquid at temperatures below 100 °C, specifically composed of a combination of organic cations and organic/inorganic anions. They present a wide liquid range together with good characteristic properties: high thermal and chemical stability, low volatility, significant electrical conductivity, high polarity, and great to dissolve an extensive range of compounds [1]. This makes them suitable for a wide variety of applications in different areas: catalytic organic transformations [2], such as lubricants; heat transfer fluids in biocatalysis [3]; biomedical and pharmaceutical applications [3]; separation and extraction processes [4]; as well as biotechnology [5] and nanoscience [6], as ideal electrolytes for use in a great number of electrochemical devices [7] such as batteries, capacitors, fuel cells, and solar cells [8]; biomolecule sensing [9,10]; explosives [11]; the determination of gas compounds [11,12]; and the development of sensors [13–15].

One of the most highly studied gases is carbon dioxide, because of the increasing levels found in the atmosphere owing to the increase in industrial activity. Carbon dioxide occurs in the combustion of fossil fuels and is considered one of the gases that contributes to the global warming of the planet. This makes the accurate, continuous monitoring of CO_2 levels a matter of necessity [16]. It is also important in medicine [17], clinical and biological research [18], industrial and biotechnological processes [19,20], and in intelligent

packaging [21]. In this respect, the growth of sensors with raised sensitivity and selectivity capable of detecting and quantifying CO_2 gas reversibly and economically is highly useful.

Ionic liquids have more CO_2 holding capacity than polymeric materials, and CO_2 can be reversibly dissolved in imidazolium-based ionic liquids [22]. Ionic liquid-based CO_2 optical sensors [23] and electrochemical sensors [24] have been developed. CO_2 is reversibly soluble in imidazolium-based ionic liquids [25], and this gas is more soluble than ethane, methane, oxygen, nitrogen, argon, hydrogen and carbon monoxide in 1-ethyl-3-methylimidazolium tetrafluoroborate ($EMIMBF_4$) [26].

$EMIMBF_4$ has been used in CO_2 gas sensors in different ways, for example, with filled photonic crystal fibres to detect the presence of CO_2 by optical transmission [27] with an ion pair formed of 1-hydroxy-3,6,8-pyrenetrisulfonate (HPTS) in an ethyl cellulose matrix to provide longer storage time, enhanced repeatability and dynamic range. However, the sensor has relatively lower sensitivity, between 0 and 5% CO_2, so it is unsuitable for monitoring CO_2 in physiologically relevant [28], and the high response and recovery time, in the order of minutes [29]. Recently our research group found an improvement that involves including ionic liquids in sensing membranes for the determination of gaseous carbon dioxide in fluorescent optical sensors [30].

Two types of sensors are commercially available for the determination and continuous monitoring of CO_2. The first is based on metal oxide semiconductors, which are relatively inexpensive compared with other sensing technologies, offering fast and robust responses, although most of these sensors have a working range from 2000 to 10,000 ppm. Responses to low CO_2 concentrations are required in many applications, such as environmental operations, disease control and diagnosis and smart packaging [31]. The second employs non-dispersive infrared sensors (NDIR) [32]. The main limitation with this type of sensor is that the miniaturization possibilities are limited when a measurement using very small volumes is needed.

Optical CO_2 sensors are a promising alternative for portable devices, as they have a comparably small sensing component. Additionally, the optoelectronic reader can be separate, increasing the possible applications. One of the problems with optical sensors for CO_2 is the response and recovery time, which are usually high. In this article, this problem is addressed through the introduction of an ionic liquid in the optical membrane that works in the near infrared region [33], reducing these times. The measurement in the NIR region has a number of advantages, including low light scattering, a drastic reduction in autofluorescence, the availability of excitation sources and low-cost photodetectors [34]. Moreover, including an ionic liquid improves the useful life of the sensor and the response and recovery time. In this way, sensors are obtained that increased the sensitivity of CO_2 monitoring, using lower amounts of reagents. Subsequently, they can be included in devices adapted for applications in the environment, clinics, and in smart packaging.

2. Experimental Section

2.1. Reagents and Materials

Hydroxypropyl methylcellulose (HPMC, Methocel E-5, LV USP/EP premium grade) (Dow Chemical Iberia S.L., Tarragona, Spain), 9004-65-3, was used as the membrane polymer. 1-Ethyl-3-methylimidazolium tetrafluoroborate (EMIMBF4), 143314-16-3, was used as IL; tetramethylammonium hydroxide pentahydrate (TMAOH), 10424-65-4, as the phase transfer agent; and Tween 20, 9005-64-5, as the surfactant, all sourced from Sigma. Microcrystalline Cr(III)-doped gadolinium aluminium borate (GAB) powder was synthesized according to [35] using the solution combustion technique, and azaBODIPY was synthesized according to [36,37] and characterized according to [33]. Sheets of Mylar-type polyester from Goodfellow (Cambridge, UK) were used as the support for the membranes.

The standard mixtures to characterize the sensing membranes were prepared using N_2 as the diluting gas, controlling the flow rates of the high purity CO_2 and N_2 gases that enter the mixing chamber with computer-controlled mass flow controllers (Air Liquide

España S.A., Madrid, Spain). The system worked at a total pressure of 760 Torr and a flow rate of 500 $cm^3 \cdot min^{-1}$.

2.2. Sensing Membrane Preparation

The sensing membrane for CO_2 contains 0.5 mg azaBODIPY dissolved in 0.5 mL of ethanol, 1 mL of HPMC 1% in water, 5 µl of Tween 20, 5 µL of a TMAOH solution containing 14 mg TMAOH in 1 mL 1:1 ethanol:water, 6 µL IL, and 1.5 mg GAB.

The CO_2 sensor consists of only one membrane prepared by casting 25 µL of the solution indicated above on a Mylar support using a spin-coating technique and then, adding 1.5 mg of GAB, leaving the microcrystals of the salt retained on the surface of the sensing zone. The membrane was then left to dry in the darkness in a box for 6 h at room temperature (20 °C) and humidity (55% relative humidity (RH)). The prepared membranes have a calculated thickness approximately of 2 µm.

2.3. Instrumentation

Cary Eclipse Varian Inc. (Palo Alto, CA, USA) luminescence spectrometer steady-state luminescence measurements were used as the analytical parameter to study the CO_2 sensing membranes. A homemade cell holder composed of two metallic triangular prisms was used to make the measurement [38] that supports the membrane, measuring the membrane by reflection at a 60° angle in the cell. This is because sensing membranes that include solid GAB show low transparency. The fluorescence of the membranes was measured with excitation and emission slit widths of 2.5 and 5 nm, λ_{ex} = 620 nm and λ_{em} = 731 nm, respectively. All measurements were made in triplicate to check for experimental errors.

In order to prepare the gas standard mixtures of CO_2 gas to characterize the membranes were used with computer-controlled mass flow controllers (Air Liquide España S.A.), operating at a total pressure of 760 Torr and a gas flow rate between 100 and 500 $cm^3 \cdot min^{-1}$, controlling the flow rates of the high purity CO_2 and N_2 (as the diluting gas) gases that enter the mixing chamber. A standard of 5% CO_2 in nitrogen was used to prepare the gas mixtures with a CO_2 concentration lower than 0.4%, with the lowest CO_2 concentration tested being 0.02%.

Temperature and humidity have an appreciable effect on the sensitivity of CO_2 sensors based on its acid-base character [39].

In order to establish different humidity conditions (from 10% to 100% RH), a controlled evaporation and mixing system (CEM) was used, consisting of a CEM three-way mixing valve and evaporator for control of the liquid source, a mass flow meter for liquid (MiniCoriflow) with a range from 0.4 to 20 $g \cdot h^{-1}$ of liquid (water in this case), and a mass flow for measurement and control of the carrier gas flow (N_2 gas). The liquid is mixed with the carrier gas flow, and both are heated with a temperature controlled heat-exchanger, resulting in the total complete evaporation of the liquid (100 °C was selected for water).

3. Results and Discussion

3.1. CO_2 Sensing Scheme

All the reagents are dissolved in an aqueous solution of HPMC as the polymeric matrix. The luminophore, GAB, is excited in the red (λexc. 620 nm in the HPMC membrane), showing a broad emission in the NIR (λems. 731 nm in the HPMC membrane). Its luminescence decay time is about 85 µs and it shows high chemical and photochemical inertness. The pH indicator is an azaBODIPY with a pKa value suitable for gaseous CO_2 determination. Also included is a hydrophobic quaternary ammonium hydroxide, in this case TMAOH, which acts as an internal buffering system to turn the pH indicator into the deprotonated form, stabilized as a hydrated ion pair:

$$TMA^+BP^- \times \ xH_2O + CO_2 \xrightarrow{K} TMA^+HCO_3^-(x-1)H_2O \times HBP \quad (1)$$

where $TMA^+BP^- \times xH_2O$ is the ion pair formed between the tetramethylammonium cation TMA^+ and the deprotonated form of azaBODIPY, BP^- and K is the equilibrium constant. In the presence of CO_2 gas, the protonated form of the azaBODIPY is formed, reducing the attenuation of the GAB luminescence, with an increase in the luminescent signal. The overlapping between the GAB spectrum (donor) and the azaBODIPY spectrum (acceptor) emission was reduced by the increase in the CO_2 concentration, increasing the fluorescent signal.

The working mechanism is based on an inner filter effect [33] similar to the sensor without IL because there was no change in the decay time within the full range of CO_2 concentrations. Consequently, the presence of IL in the sensing membrane fundamentally contributes to improving the sensitivity of the sensor and improving its characteristics [30].

3.2. Membrane Composition

The CO_2 sensing ability of these membranes is based on the luminescence quenching of a luminophore by one of the forms of an azaBODIPY-type non-fluorescent pH indicator present in a membrane that also contains TMAOH acting as an internal buffer. The change in the position of the acid-base equilibrium by the CO_2 and the concomitant change in colour result in a change in luminescence emission due to the overlap of the absorption spectrum of the basic form of the pH indicator and the emission of the luminescent GAB. CO_2 diffuses through the HPMC, dissolves and reacts with TMAOH, and gradually displaces the equilibrium of the indicator towards its acid form with a concomitant increase in the phosphorescent emission of GAB by an inner filter process [33].

Of the known ionic liquids, $EMIMBF_4$ was selected for its good solubility in aqueous media and good characteristics for CO_2 sensing [30]. Thanks to the presence of both species in the solution, the amount of TMAOH needed to deprotonate azaBODIPY and change it to its basic form is considerably small. It has also been reported that in the presence of the ionic liquid anion ($[BF4]^-$), the anion that would decompose into HF and F^-, which would catalyse the formation of hydrogen carbonate, stimulating the hydration of CO_2 and its posterior protolysis [28].

The amount of pH indicator was set at 0.5 mg. The initial sensing membrane without the inclusion of $EMIMBF_4$ was prepared with a 2% HPMC polymer, the minimum concentration to produce a membrane with the required mechanical properties and a good response. However, it was observed that, after adding the ionic liquid, the optical and mechanical characteristics of the membrane worsened. Therefore, the percentage of HPMC had to be reduced considerably. Different membranes were prepared with percentages of HPMC in the range of 1.0 to 2.0% *w*/*w*. In each case, the maximum response was reached when the percentage of HPMC was 1.0% *w*/*w* and this value was selected as optimal for successive experiments (Figure 1a).

The amount of the TMAOH transfer agent phase was optimized preparing different membranes with TMAOH contents from 0 to 1.8% *w*/*w*. With small amounts of TMAOH, the difference between I_{100}-I_0 is very small because there is not enough TMAOH for all the azaBODIPY to be in its basic form, preventing the membrane from responding to CO_2. Similarly, when the TMAOH concentration is too high (1.8% *w*/*w*), the pH is too basic and the sensitivity is low. The maximum signal was obtained with 0.75% TMAOH (Figure 1b).

To optimize the amount of $EMIMBF_4$ in the sensing membrane, eight different sensors were prepared with amounts ranging from 0.5% to 4.3% *w*/*w*. Figure 1c shows that the best result was obtained for 1.5% *w*/*w*. The inclusion of surfactants in the membrane increases the response of the sensor and the preparation of the membranes is improved by spin coating. The surfactant selected was Tween 20, because of its effectiveness with this sensing membrane over the other surfactants tested [30,40]. To study the influence of Tween 20, different membranes were prepared containing between 0 and 1.15% *w*/*w*. In all cases, the maximum signal was obtained for 0.38% *w*/*w*; this amount was thus selected.

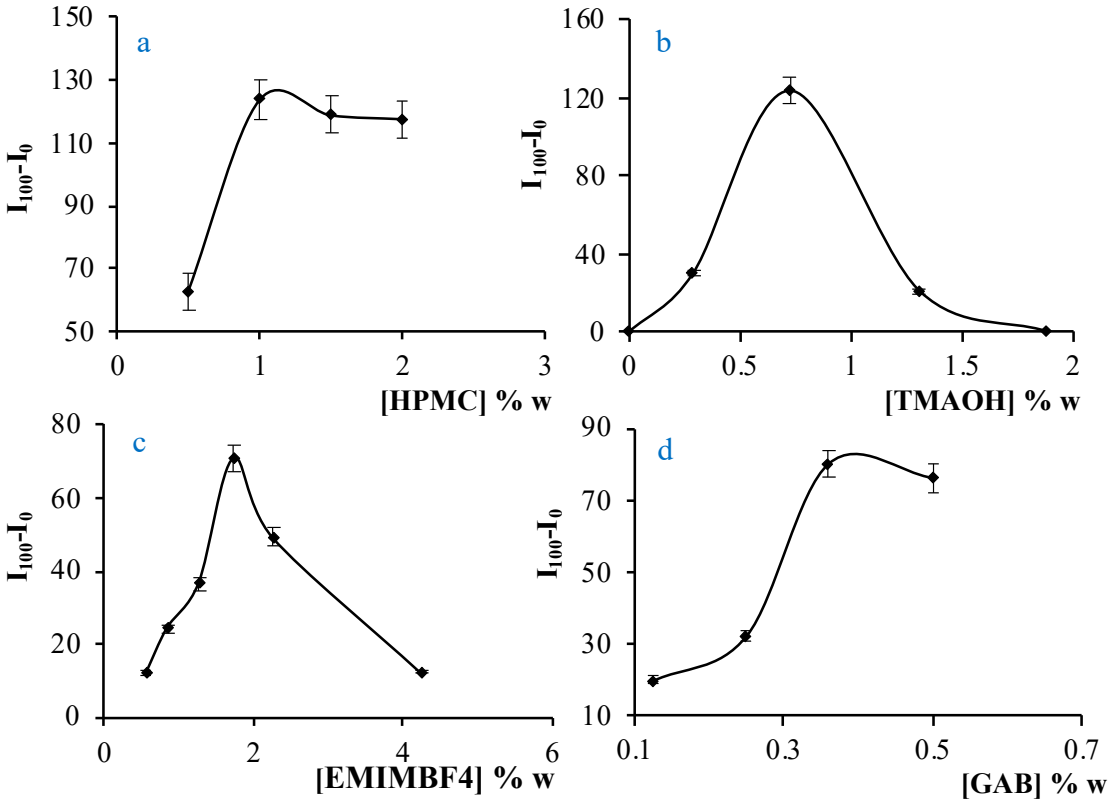

Figure 1. Optimization of reagent concentration for sensing membrane containing IL: (**a**) HPMC; (**b**) TMAOH; (**c**) $EMIMBF_4$; (**d**) GAB.

The optimization of the amount of GAB was made taking into account the I_{100}-I_0 parameter and the response and recovery times, as the goal was to obtain the maximum signal in the shortest possible time. Table 1 shows the results of the optimization of GAB.

Table 1. Optimization of the amount of GAB versus three variables: I_{100}-I_0 parameter, response time and recovery time.

GAB (% *w*/*w*)	0.12	0.25	0.35	0.5
I_{100}-I_0	20.0	32.4	80.2	76.2
t_{90} (s)	16	30	23	52
t_{10} (s)	32	32	29	63

For 0.12 and 0.25% *w*/*w* of GAB, the values of I_{100}-I_0 are very similar, but the response and recovery times improve for 0.12% of GAB. For 0.5% *w*/*w* of GAB, the response time is very fast, but the parameter I_{100}-I_0 is too small to be considered adequate to work with. The amount of 0.35% *w*/*w* of GAB was selected as the optimum value in the end (Figure 1d).

It is well known that temperature and humidity have a considerable effect on the sensitivity of luminescent sensors [41], particularly at high values of both parameters. The dependence of the relative humidity of the sensing membrane at room temperature (22 ± 1 °C) was studied, obtaining the calibration function at relative humidities between 10% and 100% and observing a reduction in sensitivity with as the % RH increases (Figure 2). The experiments assays were carried out at a constant room temperature, 22 ± 1 °C, in all cases, although there is a known decrease in sensitivity as the temperature increases [42]. This fact occurs owing to the opposite dependence of CO_2 solubility in the pH indicator membrane on the temperature [43].

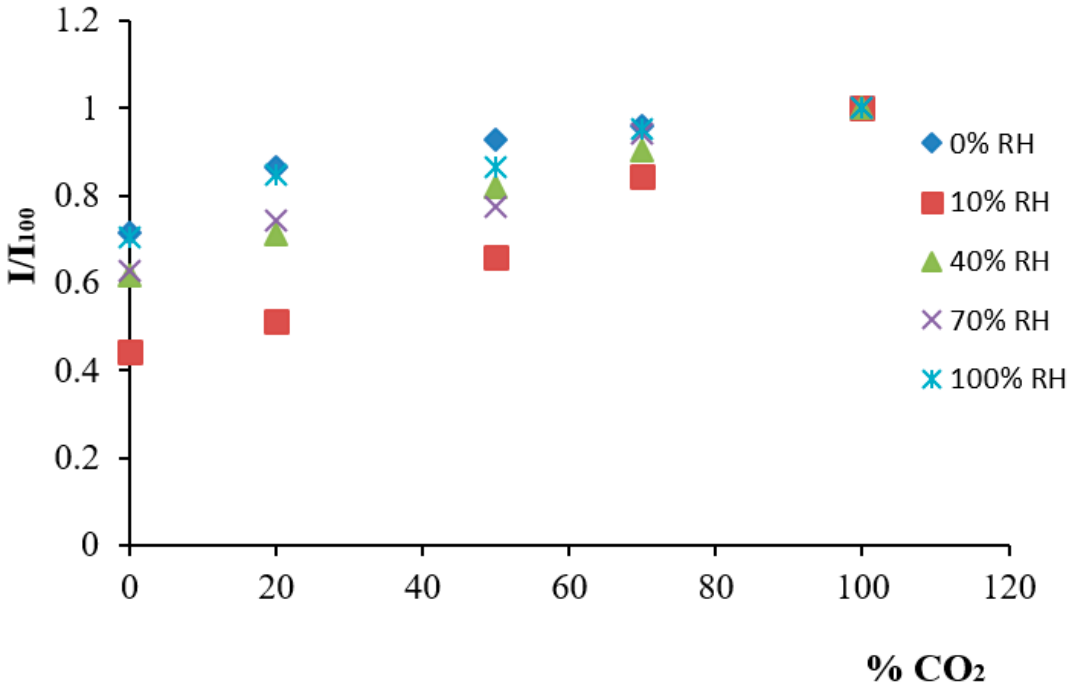

Figure 2. Humidity dependence of the sensing membrane: ◆: 0% RH; ■: 10% RH; ▲: 40% RH; ×: 70% RH; ✳: 100% RH.

In order to study the effect of different concentrations gases, such as O_2 and H_2, and the minor constituents, such as SO_2, HCl, and CH_4, were exposed to the sensing membrane It was concluded that only gases with acid-base properties, like HCl and SO_2, produce a strong interference, as expected owing to the sensing mechanism, while other gaseous species such as CH_4 and O_2 did not produce any change in the signal when present.

3.3. Analytical Characterization of the Sensing Membranes

The hyperbolic response of both colorimetric and luminescent CO_2 sensors between the measured signal and CO_2 concentration is well known [44–46]. Different approaches have been used to linearize the experimental data, such as the Stern-Volmer equation [47] and the equation proposed by Nakamura and Amao [48]. In this case, the calibration function (Figure 3) was obtained using Equation (1), because of the good fit for linearizing the experimental data. Each measurement was obtained as a mean value of three replicates covering the whole range of concentrations working at room temperature (22 ± 1 °C):

$$y = a + bx^c \quad (2)$$

where the values of the coefficients are as follows: a = 0.72 ± 0.05; b = 0.12 ± 0.05; c = 0.17 ± 0.05 and r^2 = 0.9961. The signal increases exponentially until it reaches 100% CO_2. For that reason, the detection limit, LOD, was calculated from the raw exponential experimental data by using the first three points (Figure 3 insert), which can be adjusted to a straight line, I/I_{100} = 0.0051[% CO_2] + 0.856; R^2 = 0.989 [49], using (LOD = $t_0N - 3s_0$), where t_0N is the blank or average value in the absence of CO_2 and s_0 is the critical level or standard deviation of the blank, which was calculated from six replicate measurements. The limit of quantification (LOQ) of the instrumental procedure was obtained from the linear Stern-Volmer calibration function by using LOQ = $t_0N + 10s_0$. The LOD found with this approach was 0.26% CO_2 and the LOQ was 1.64% CO_2.

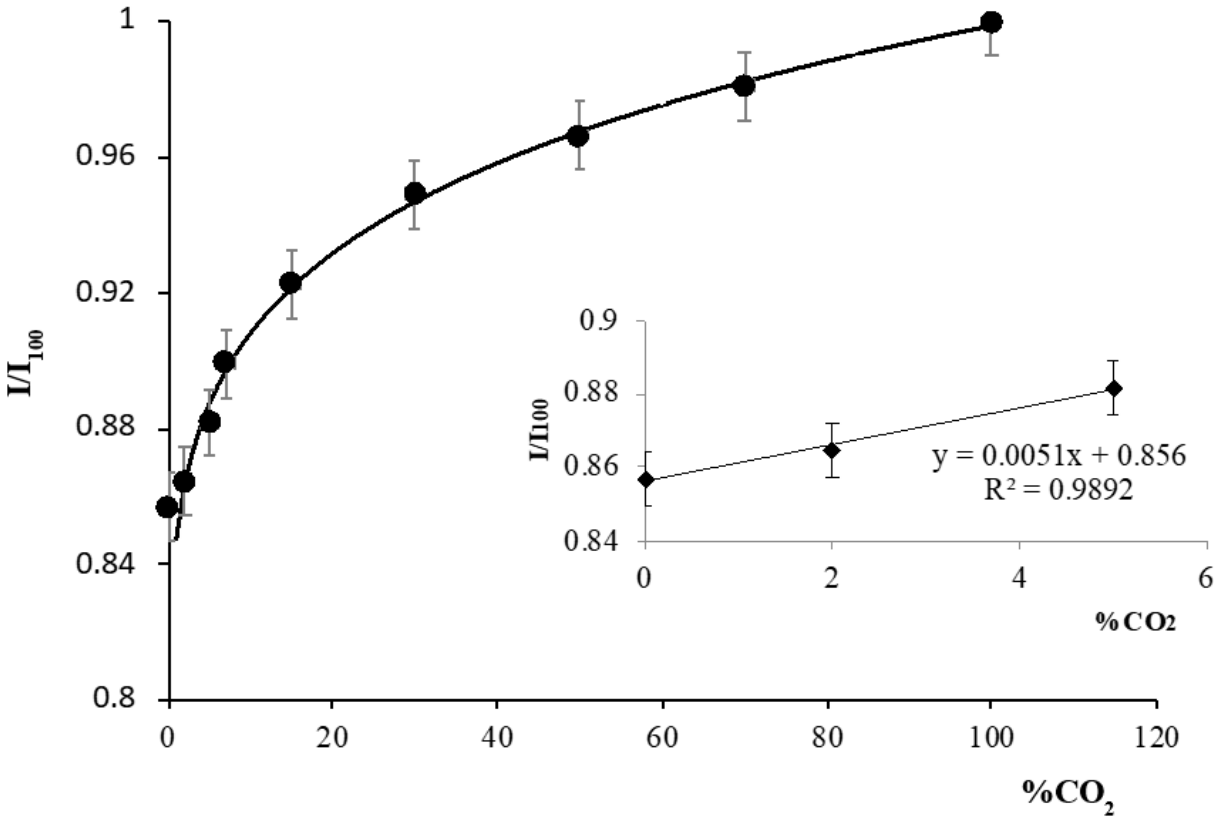

Figure 3. Sensor response to CO_2 concentration. Insert: linearization of the first three experimental raw data for LOD and LQD calculation.

The precision was evaluated at two CO_2 concentrations (0.6% and 16.7%), performing 15 measurements each and obtaining relative standard deviations. Comparing the results to those obtained using other sensors described by us [30] that include ionic liquids in their composition, we found that the relative standard deviations in both cases are lower than 5%. For the proposal of determining the reversibility of the sensor, alternative atmospheres of pure CO_2 and pure nitrogen with a response time between 10% and 90% of the maximum signal and a recovery time from 90% to 10% were exposed on the sensing membrane. In Figure 4, one can observe no hysteresis during the measurements as well as the fact that the signal change was fully reversible.

The stability of the membrane was studied by measuring the I_{100}-I_0 value for 10 months from a set of membranes using a Shewhart control chart. We defined the lifetime of the sensor (T1) as that in which the sensor output signal remains within the control line on the Shewhart chart for one constant concentration of CO_2 gas concentration. The lifetime of the sensing membrane (T2) is the time during which the membrane responds to CO_2, even though it is necessary to recalibrate it. Figure 5 shows the control chart for the sensing membrane containing IL. The sensor signal remains within the established control limits up to 20 days, after which the sensor responds up to 300 days, as it is possible to recalibrate the signal within this period. After this period, the sensor must be replaced because no response is obtained.

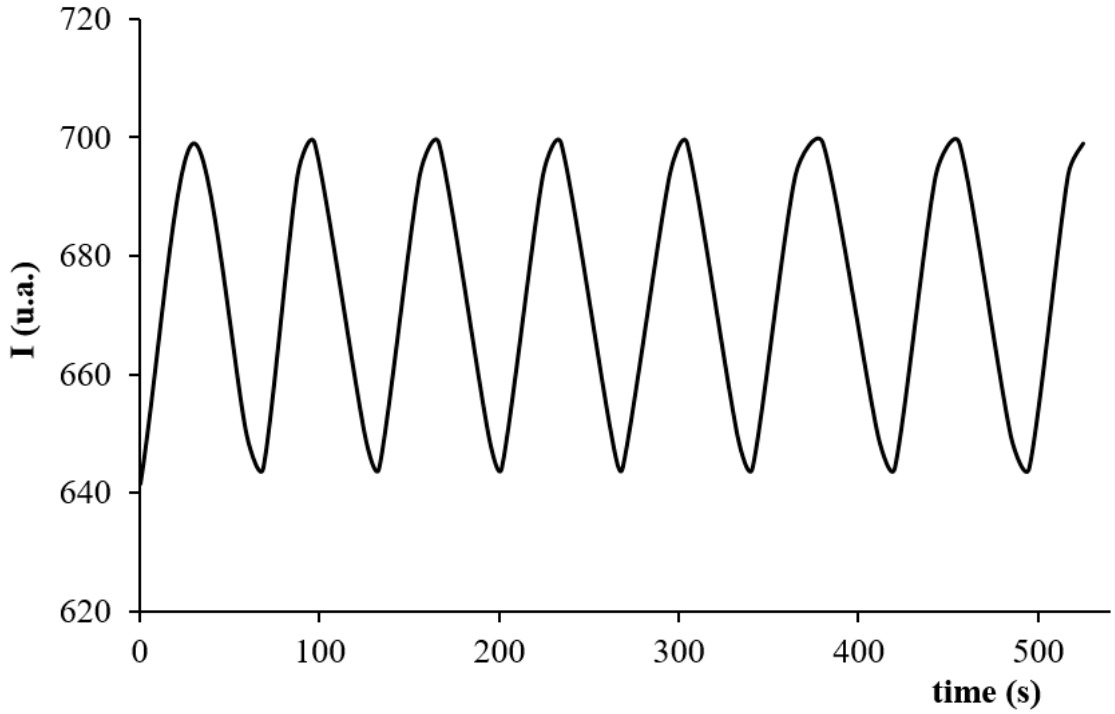

Figure 4. Response and recovery time of CO_2 sensing membrane while increasing and decreasing CO_2 concentrations (from 10% to 90% and vice-versa).

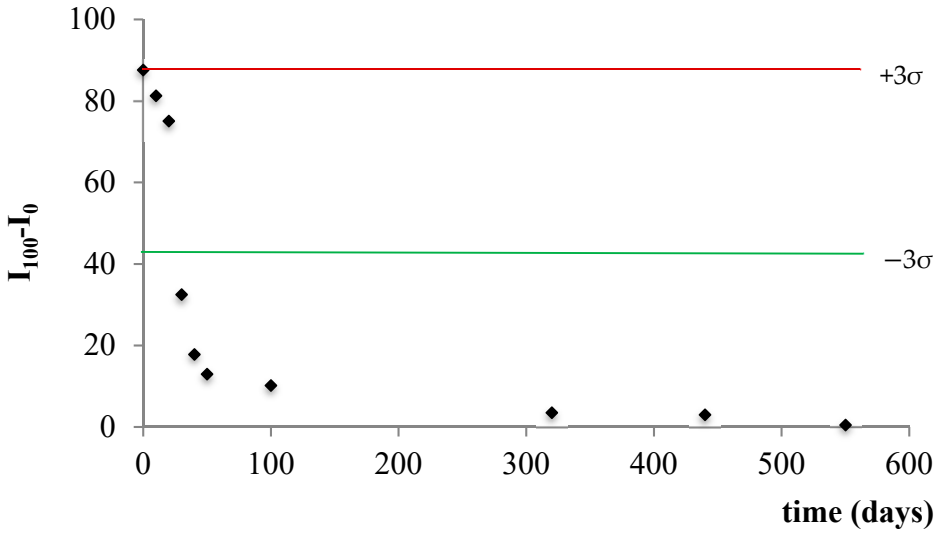

Figure 5. Shewhart control chart for sensing membrane lifetime.

Table 2 shows the comparison of the analytical characteristics of the sensing membrane proposed here versus the sensing membrane without IL [33]. We observed an improvement in the LOD for the membranes containing IL (from 0.57% to 0.26%). The precision measured at two CO_2 levels (0.6% and 16.7% CO_2) was better when using IL. The biggest difference in performance characteristics was related to response time. The membrane with IL reduced the response time t_{90} to 38% (from 60 s to 23 s) and recovery time t_{10} to 34% (from 120 s to 49 s).

Table 2. Comparison of the analytical characteristics of sensing membranes for CO_2 determination with and without IL.

Analytical Parameter	azaBODIPY without IL	azaBODIPY with IL
I_{100}-I_0	140.7	87.6
Slope	15.9 ± 0.8	0.0051 ± 0.01
Intercept	0.6 ± 0.163	0.9 ± 0.10
R^2	0.999	0.982
LOD (%CO_2)	0.57	0.26
LDQ (%CO_2)	1.7	1.64
Upper limit (%CO_2)	60	100
Detection interval (%CO_2)	0.57–1.7	0.26–1.64
Quantification Interval (%CO_2)	1.7–60	1.64–100
Precision (RSD; n = 15) at 0.6% CO_2	1.23	0.70
Precision (RSD; n = 15) at 16.7% CO_2	0.62	3.0
Response time (t_{90}) (s)	60 ± 2	23 ± 2
Recovery time (t_{10}) (s)	120.0 ± 0,6	49 ± 1
T1 (days)	6	20
T2 (days)	570	120
Storage	In dark container	In dark container

The lifetime (T1) of the sensor with IL is higher than the reference T1 value (15 days), noting once again that including IL increases the lifetime. Table 3 summarizes the principal analytical characteristics of the CO_2 gas sensor with IL in its composition found in the literature. The fluorescent pH indicator 1-hydroxypyrene3,6,8-trisulfonate (HPTS) (τ0~5 ns) has been widely used with this type of sensor to analyse carbon dioxide gas. Additionally, it was the first to include an ionic liquid in diverse polymeric matrices such as ethyl cellulose, poly(methyl methacrylate), prepared on an inert Mylar support or using an electrospinning technique. Other indicators such as α-naphtholphthalein and azaBODIPY have also been used in different matrices, as in this case, and the response time and recovery time are considerably improved compared with the rest of the sensors developed to date. Additionally, the precision, as RSD (%), is significantly lower for the proposed sensor than for those developed previously, although it does not have the lowest LOD of all the sensors.

The inclusion of ionic liquids, together with an azaBODIPY forming sensing membrane, in this study, considerably improves the detection limit and response time of the sensor, with its response in the near-infrared (NIR) region. It has several advantages, including low light scattering, dramatically reduced autofluorescence and the availability of low-cost photodetectors and excitation sources.

Table 3. Performance comparison of CO_2 sensing membranes based on IL.

Sensing Chemistry	Technique	LOD (% CO_2)	t_{90}–t_{10} (s)	Precision RSD (%)	Lifetime (Days)/Storage	Ref
HPTS/EC/IL	I	-	54–180	-	95	[28]
HPTS/EC/TOABr/TOAOH/IL HPTS/PMMA/TOABr/TOAOH//IL	I	-	15–120 20–300	-	210/ambient	[50]
PtOEP/N/IL/HPMC/PVCD	I	0.008	10–48.5	0.21	280/ambient	[30]
PAVB/IL	I	0.0286	127–177	-	-	[23]
HEC/MCP/IL	A	0.36	530–540	-	14/ambient	[15]
HPMC/N/IL	PD	0.005	1.3–2.5	1.5	30/ambient	[30]
azaBODIPY/GAB/IL/HPMC	I	0.26	23–49	0.7	20/ambient	Current study

HPTS: 1-Hydroxy-3,6-8 pyrenetrisulfonate; EC: Ethyl cellulose; IL: Ionic liquid; PMMA: Poly (methyl methacrylate); TOAOH: Tetraoctylammonium hydroxide; PAVB: Poly(1-allyl-3-vinylimidazolium bromide; HEC: 2-Hydroxyethyl cellulose; MCP: Meta cresol purple sodium salt; PtOEP: Platinum octaethylporphyrin complex; N: α-Naphtholphthalein; PVCD: Poly(vinylidene chloride-co-vinyl chloride); aB: azaBODIPY; GAB: Cr(III)-doped gadolinium aluminium borate; HPMC: Hydroxypropyl methylcellulose; I: Fluoresence intensity, A: Absorbance; PD: Platform Dedicated.

4. Conclusions

In this study, we report the development of a CO_2 sensing membrane that operates with an inner filter process and in which a very stable inorganic phosphor and an ionic liquid were included for extremely fast CO_2 capture. This considerably improves both the sensitivity of the sensor and its response and recovery time to determine and monitor CO_2 in the infrared region.

A significant improvement on an NIR optical sensor based on azaBODIPY is obtained for the determination of gaseous CO_2 using the measurement of the fluorescence intensity of the GAB nanoparticles included in the HPMC membrane with TMAOH as a phase transfer agent and $EMIMBF_4$ as IL by shifting the acid-base equilibrium of the included azaBODIPY. The advantages of working in the NIR region combined with those of including an ionic liquid, that is, improvements in sensitivity (LOD 0.26%), precision (RSD less than 0.5%) and response and recovery times (t_{90} 23 s and t_{10} 49 s) and useful life (20 days), make this sensor especially attractive for application in biological systems.

The sensor can be included in specific instrumentation for application in the environment, diagnostics and disease tracking and smart packaging, all goals for future research.

Author Contributions: Conceptualization, M.D.F.-R.; Methodology, M.D.F.-R., and F.M.-M.; Formal Analysis, M.D.F.-R., and F.M.-M.; Investigation, M.D.F.-R., F.M.-M., and I.M.P.d.V.-S.; Resources, M.D.F.-R., F.M.-M., I.M.P.d.V.-S., and L.F.C.-V.; Data Curation, M.D.F.-R. and I.M.P.d.V.-S.; Writing-Original Draft Preparation, M.D.F.-R. and L.F.C.-V.; Writing-Review and Editing, M.D.F.-R., I.M.P.d.V.-S., and L.F.C.-V.; Visualization, M.D.F.-R.; Supervision, M.D.F.-R. and I.M.P.d.V.-S.; Project Administration, L.F.C.-V.; Funding Acquisition, L.F.C.-V. All authors have read and agreed to the published version of the manuscript.

Funding: This work was founded by Spanish "Ministerio de Economía y Competitividad" (Projects PID2019-103938RB-I00 and CTQ2017-86125-P) and Junta de Andalucía (Projects B-FQM-243-UGR18 and P18-RT-2961). The projects were partially supported by European Regional Development Funds (ERDF).

Institutional Review Board Statement: Not applicable.

Informed Consent Statement: Not applicable.

Data Availability Statement: Data is contained within the article.

Acknowledgments: The authors would like to acknowledge Antonio Rodríguez Diéguez and Francisco Santoyo González for their help in the synthesis of gadolinium salt and azaBODIPY, respectively.

Conflicts of Interest: The authors declare no conflict of interest.

References

1. Greaves, T.L.; Drummond, C.J. Protic Ionic Liquids: Properties and Applications. *Chem. Rev.* **2008**, *108*, 206–237. [CrossRef]
2. Vekariya, R.L. A review of ionic liquids: Applications towards catalytic organic transformations. *J. Mol. Liq.* **2017**, *227*, 44–60. [CrossRef]
3. Gao, W.-W.; Zhang, F.-X.; Zhang, G.-X.; Zhou, C.-H. Key factors affecting the activity and stability of enzymes in ionic liquids and novel applications in biocatalysis. *Biochem. Eng. J.* **2015**, *99*, 67–84. [CrossRef]
4. Delgado-Mellado, N.; Ovejero-Perez, A.; Navarro, P.; Larriba, M.; Ayuso, M.; García, J.; Rodríguez, F. Imidazolium and pyridinium-based ionic liquids for the cyclohexane/cyclohexene separation by liquid-liquid extraction. *J. Chem. Thermodyn.* **2019**, *131*, 340–346. [CrossRef]
5. Claus, J.; Sommer, F.O.; Kragl, U. Ionic liquids in biotechnology and beyond. *Solid State Ion.* **2018**, *314*, 119–128. [CrossRef]
6. Arumugam, V.; Redhi, G.; Gengan, R.M. Chapter 12—The application of ionic liquids in nanotechnology. In *Fundamentals of Nanoparticles*; Barhoum, A., Hamdy Makhlouf, A.S., Eds.; Elsevier: Amsterdam, The Netherlands, 2018; pp. 371–400. [CrossRef]
7. Liu, H.; Yu, H. Ionic liquids for electrochemical energy storage devices applications. *J. Mater. Sci. Technol.* **2019**, *35*, 674–686. [CrossRef]
8. Martins, V.L.; Torresi, R.M. Ionic liquids in electrochemical energy storage. *Curr. Opin. Electrochem.* **2018**, *9*, 26–32. [CrossRef]
9. Rostami, S.; Mehdinia, A.; Jabbari, A.; Kowsari, E.; Niroumand, R.; Booth, T.J. Colorimetric sensing of dopamine using hexagonal silver nanoparticles decorated by task-specific pyridinum based ionic liquid. *Sens. Actuators B Chem.* **2018**, *271*, 64–72. [CrossRef]
10. Rauf, S.; Nawaz, M.A.H.; Muhammad, N.; Raza, R.; Shahid, S.A.; Marty, J.L.; Hayat, A. Protic ionic liquids as a versatile modulator and stabilizer in regulating artificial peroxidase activity of carbon materials for glucose colorimetric sensing. *J. Mol. Liq.* **2017**, *243*, 333–340. [CrossRef]
11. Yu, H.A.; DeTata, D.A.; Lewis, S.W.; Silvester, D.S. Recent developments in the electrochemical detection of explosives: Towards field-deployable devices for forensic science. *TrAC Trends Anal. Chem.* **2017**, *97*, 374–384. [CrossRef]
12. Akhmetshina, A.I.; Gumerova, O.R.; Atlaskin, A.A.; Petukhov, A.N.; Sazanova, T.S.; Yanbikov, N.R.; Nyuchev, A.V.; Razov, E.N.; Vorotyntsev, I.V. Permeability and selectivity of acid gases in supported conventional and novel imidazolium-based ionic liquid membranes. *Sep. Purif. Technol.* **2017**, *176*, 92–106. [CrossRef]
13. Baltes, N.; Beyle, F.; Freiner, S.; Geier, F.; Joos, M.; Pinkwart, K.; Rabenecker, P. Trace detection of oxygen—ionic liquids in gas sensor design. *Talanta* **2013**, *116*, 474–481. [CrossRef] [PubMed]
14. Gao, L.; Yang, X.; Shu, Y.; Chen, X.; Wang, J. Ionic liquid-based slab optical waveguide sensor for the detection of ammonia in human breath. *J. Colloid Interface Sci.* **2018**, *512*, 819–825. [CrossRef] [PubMed]
15. Perez de Vargas-Sansalvador, I.M.; Erenas, M.M.; Diamond, D.; Quilty, B.; Capitan-Vallvey, L.F. Water based-ionic liquid carbon dioxide sensor for applications in the food industry. *Sens. Actuators B Chem.* **2017**, *253*, 302–309. [CrossRef]
16. Behera, K.; Pandey, S.; Kadyan, A.; Pandey, S. Ionic Liquid-Based Optical and Electrochemical Carbon Dioxide Sensors. *Sensors* **2015**, *15*, 30487–30503. [CrossRef] [PubMed]
17. Kapurch, C.J.; Abcejo, A.S.; Pasternak, J.J. The relationship between end-expired carbon dioxide tension and severity of venous air embolism during sitting neurosurgical procedures—A contemporary analysis. *J. Clin. Anesth.* **2018**, *51*, 49–54. [CrossRef]
18. Laporte-Uribe, J.A. The role of dissolved carbon dioxide in both the decline in rumen pH and nutritional diseases in ruminants. *Anim. Feed Sci. Technol.* **2016**, *219*, 268–279. [CrossRef]
19. Lin, B.; Benjamin, N.I. Determinants of industrial carbon dioxide emissions growth in Shanghai: A quantile analysis. *J. Clean. Prod.* **2019**, *217*, 776–786. [CrossRef]
20. Yu, M.; Sediq, A.S.; Zhang, S.; Nejadnik, M.R.; Every, H.A.; Jiskoot, W.; Witkamp, G.-J. Towards the development of a supercritical carbon dioxide spray process to coat solid protein particles. *J. Supercrit. Fluids* **2018**, *141*, 49–59. [CrossRef]
21. Puligundla, P.; Jung, J.; Ko, S. Carbon dioxide sensors for intelligent food packaging applications. *Food Control* **2012**, *25*, 328–333. [CrossRef]
22. Soriano, A.N.; Doma, B.T.; Li, M.-H. Solubility of Carbon Dioxide in 1-Ethyl-3-methylimidazolium Tetrafluoroborate. *J. Chem. Eng. Data* **2008**, *53*, 2550–2555. [CrossRef]
23. Wu, J.; Yin, M.-J.; Seefeldt, K.; Dani, A.; Guterman, R.; Yuan, J.; Zhang, A.P.; Tam, H.-Y. In Situ μ-printed optical fiber-tip CO_2 sensor using a photocrosslinkable poly(ionic liquid). *Sens. Actuators B Chem.* **2018**, *259*, 833–839. [CrossRef]
24. Revsbech, N.P.; Garcia-Robledo, E.; Sveegaard, S.; Andersen, M.H.; Gothelf, K.V.; Larsen, L.H. Amperometic microsensor for measurement of gaseous and dissolved CO_2. *Sens. Actuators B Chem.* **2019**, *283*, 349–354. [CrossRef]
25. Aki, S.N.V.K.; Mellein, B.R.; Saurer, E.M.; Brennecke, J.F. High-Pressure Phase Behavior of Carbon Dioxide with Imidazolium-Based Ionic Liquids. *J. Phys. Chem. B* **2004**, *108*, 20355–20365. [CrossRef]
26. Jacquemin, J.; Costa Gomes, M.F.; Husson, P.; Majer, V. Solubility of carbon dioxide, ethane, methane, oxygen, nitrogen, hydrogen, argon, and carbon monoxide in 1-butyl-3-methylimidazolium tetrafluoroborate between temperatures 283 K and 343 K and at pressures close to atmospheric. *J. Chem. Thermodyn.* **2006**, *38*, 490–502. [CrossRef]
27. Doganata, S.; Coskun, S.; Oeztuerk, Y.; Celikoglu, M. Investigation of interaction of carbon dioxide with ionic liquid filled photonic crystal fiber. *Optoelectron. Adv. Mater. Rapid Commun.* **2016**, *10*, 354–357.
28. Oter, O.; Ertekin, K.; Derinkuyu, S. Ratiometric sensing of CO_2 in ionic liquid modified ethyl cellulose matrix. *Talanta* **2008**, *76*, 557–563. [CrossRef]

29. Oter, O.; Ertekin, K.; Topkaya, D.; Alp, S. Emission-based optical carbon dioxide sensing with HPTS in green chemistry reagents: Room-temperature ionic liquids. *Anal. Bioanal. Chem.* **2006**, *386*, 1225–1234. [CrossRef]
30. Fernández-Ramos, M.D.; Aguayo-López, M.L.; Pérez de Vargas-Sansalvador, I.; Capitán-Vallvey, L.F. Ionic liquids on optical sensors for gaseous carbon dioxide. *Anal. Bioanal. Chem.* **2018**, *410*, 5931–5939. [CrossRef]
31. Fine, G.F.; Cavanagh, L.M.; Afonja, A.; Binions, R. Metal oxide semi-conductor gas sensors in environmental monitoring. *Sensors* **2010**, *10*, 5469–5502. [CrossRef]
32. Hodgkinson, J.; Smith, R.; Ho, W.O.; Saffell, J.R.; Tatam, R.P. Non-dispersive infra-red (NDIR) measurement of carbon dioxide at 4.2μm in a compact and optically efficient sensor. *Sens. Actuators B Chem.* **2013**, *186*, 580–588. [CrossRef]
33. Fernández-Ramos, M.D.; Aguayo-López, M.L.; de los Reyes-Berbel, E.; Santoyo-González, F.; Capitán-Vallvey, L.F. NIR optical carbon dioxide gas sensor based on simple azaBODIPY pH indicators. *Analyst* **2019**, *144*, 3870–3877. [CrossRef] [PubMed]
34. Honeycutt, W.T.; Ley, M.T.; Materer, N.F. Precision and Limits of Detection for Selected Commercially Available, Low-Cost Carbon Dioxide and Methane Gas Sensors. *Sensors* **2019**, *19*, 3157. [CrossRef] [PubMed]
35. Borisov, S.M.; Gatterer, K.; Bitschnau, B.; Klimant, I. Preparation and Characterization of Chromium(III)-Activated Yttrium Aluminum Borate: A New Thermographic Phosphor for Optical Sensing and Imaging at Ambient Temperatures. *J. Phys. Chem. C* **2010**, *114*, 9118–9124. [CrossRef] [PubMed]
36. Jokic, T.; Borisov, S.M.; Saf, R.; Nielsen, D.A.; Kühl, M.; Klimant, I. Highly Photostable Near-Infrared Fluorescent pH Indicators and Sensors Based on BF2-Chelated Tetraarylazadipyrromethene Dyes. *Anal. Chem.* **2012**, *84*, 6723–6730. [CrossRef]
37. Gorman, A.; Killoran, J.; O'Shea, C.; Kenna, T.; Gallagher, W.M.; O'Shea, D.F. In Vitro Demonstration of the Heavy-Atom Effect for Photodynamic Therapy. *J. Am. Chem. Soc.* **2004**, *126*, 10619–10631. [CrossRef]
38. Capitán-Vallvey, L.F.; Fernández Ramos, M.D.; Avidad, R.; Deheidel, M.K.A. Determination of the pesticide morestan by means of a single-use phosphorimetric sensor. *Anal. Chim. Acta* **2001**, *440*, 131–141. [CrossRef]
39. Mills, A.; Lepre, A.; Wild, L. Breath-by-breath measurement of carbon dioxide using a plastic film optical sensor. *Sens. Actuators B* **1997**, *39*, 419–425. [CrossRef]
40. Aguayo-López, M.L.; Capitán-Vallvey, L.F.; Fernández-Ramos, M.D. Optical sensor for carbon dioxide gas determination, characterization and improvements. *Talanta* **2014**, *126*, 196–201. [CrossRef]
41. Mills, A.; Chang, Q.; McMurray, N. Equilibrium Studies on Colorimetric Plastic Film Sensors for Carbon Dioxide. *Anal. Chem.* **1992**, *64*, 1383–1389. [CrossRef]
42. Fernández-Ramos, M.D.; Moreno-Puche, F.; Escobedo, P.; García-López, P.A.; Capitán-Vallvey, L.F.; Martínez-Olmos, A. Optical portable instrument for the determination of CO_2 in indoor environments. *Talanta* **2020**, *208*, 120387. [CrossRef] [PubMed]
43. Marazuela, M.D.; Moreno Bondi, M.C.; Orellana, G. Enhanced performance of a fibre-optic luminescence CO_2 sensor using carbonic anhydrase. *Sens. Actuators B Chem.* **1995**, *29*, 126–131. [CrossRef]
44. Neurauter, G.; Klimant, I.; Wolfbeis, O.S. Microsecond lifetime-based optical carbon dioxide sensor using luminescence resonance energy transfer. *Anal. Chim. Acta* **1999**, *382*, 67–75. [CrossRef]
45. Mills, A.; Chang, Q. Fluorescence plastic thin-film sensor for carbon dioxide. *Analyst* **1993**, *118*, 839–843. [CrossRef]
46. Borisov, S.M.; Waldhier, M.C.; Klimant, I.; Wolfbeis, O.S. Optical Carbon Dioxide Sensors Based on Silicone-Encapsulated Room-Temperature Ionic Liquids. *Chem. Mater.* **2007**, *19*, 6187–6194. [CrossRef]
47. Gehlen, M.H. The centenary of the Stern-Volmer equation of fluorescence quenching: From the single line plot to the SV quenching map. *J. Photochem. Photobiol. C: Photochem. Rev.* **2020**, *42*, 100338. [CrossRef]
48. Nakamura, N.; Amao, Y. Optical sensor for carbon dioxide combining colorimetric change of a pH indicator and a reference luminescent dye. *Anal. Bioanal. Chem.* **2003**, *376*, 642–646. [CrossRef]
49. ISO. Capability of detection. Methodology in the linear and non-linear cases. In *ISO 11843-5:2008. Capability of Detection. Part 5: Methodology in the Linear and Non-Linear Calibration Cases*; International Standardization Organization: Geneva, Switzerland, 2008.
50. Aydogdu, S.; Ertekin, K.; Suslu, A.; Ozdemir, M.; Celik, E.; Cocen, U. Optical CO_2 Sensing with Ionic Liquid Doped Electrospun Nanofibers. *J. Fluoresc.* **2011**, *21*, 607–613. [CrossRef]